Wall energy relaxation in the Cahn–Hilliard model for moving contact lines

Pengtao Yue and James J. Feng

Citation: Physics of Fluids (1994-present) **23**, 012106 (2011); doi: 10.1063/1.3541806
View online: http://dx.doi.org/10.1063/1.3541806
View Table of Contents: http://scitation.aip.org/content/aip/journal/pof2/23/1?ver=pdfcov
Published by the AIP Publishing

Wall energy relaxation in the Cahn–Hilliard model for moving contact lines

Pengtao Yue[1] and James J. Feng[2]
[1]*Department of Mathematics, Virginia Polytechnic Institute and State University, Blacksburg, Virginia 24061-0123, USA*
[2]*Department of Chemical and Biological Engineering, University of British Columbia, Vancouver BC V6T 1Z3, Canada and Department of Mathematics, University of British Columbia, Vancouver BC V6T 1Z2, Canada*

(Received 19 August 2010; accepted 20 December 2010; published online 25 January 2011)

The Cahn–Hilliard model uses diffusion between fluid components to regularize the stress singularity at a moving contact line. In addition, it represents the dynamics of the near-wall layer by the relaxation of a wall energy. The first part of the paper elucidates the role of the wall relaxation in a flowing system, with two main results. First, we show that wall energy relaxation produces a dynamic contact angle that deviates from the static one, and derive an analytical formula for the deviation. Second, we demonstrate that wall relaxation competes with Cahn–Hilliard diffusion in defining the apparent contact angle, the former tending to "rotate" the interface at the contact line while the latter to "bend" it in the bulk. Thus, varying the two in coordination may compensate each other to produce the same macroscopic solution that is insensitive to the microscopic dynamics of the contact line. The second part of the paper exploits this competition to develop a computational strategy for simulating realistic flows with microscopic slip length at a reduced cost. This consists in computing a moving contact line with a diffusion length larger than the real slip length, but using the wall relaxation to correct the solution to that corresponding to the small slip length. We derive an analytical criterion for the required amount of wall relaxation, and validate it by numerical results on dynamic wetting in capillary tubes and drop spreading. © *2011 American Institute of Physics*. [doi:10.1063/1.3541806]

I. INTRODUCTION

The conventional Navier–Stokes formulation runs into a nonintegrable stress singularity at moving contact lines. Different slip models have been proposed to avoid this singularity in sharp-interface models.[1,2] Alternatively, one can use the diffuse-interface theory, also known as the phase-field theory, to regularize the singularity at the contact line.[3–5] In this approach, the Cahn–Hilliard (CH) model is used to describe the interface evolution, and the contact line moves by means of a diffusion across the interface driven by gradients of the chemical potential. More references can be found in Ref. 6.

How do we use the phenomenological CH model to simulate a real moving contact line, as in an experiment with silicone oil displacing water in a glass capillary tube? This is a complex and subtle question, a large part of which hinges on the idea of the *sharp-interface limit*. When CH is used to represent an interface that does not intersect a solid wall, as is the case for drop deformation, the sharp-interface limit is well established.[7–9] In such a limit, achieved at finite interfacial thickness ϵ, the results no longer depend on ϵ, and the diffusion across the interface becomes negligible. The results thus become comparable with sharp-interface computations and experiments, in which the interface is exceedingly thin, down to molecular scale. As long as this limit is achieved, the physical relevance of the phenomenological CH diffusion is immaterial.

CH diffusion takes on a much more important role in simulating a moving contact line; it is the agent that produces the motion of the contact line. Thus, any sharp-interface limit must preserve this diffusion so as to produce a finite contact-line speed. From numerical results, Yue *et al.*[6] demonstrated convergence toward such a limit by reducing ϵ while keeping the mobility γ, essentially the CH diffusivity, constant. In this limit, the diffuse-interface solution agrees quantitatively with the sharp-interface Cox solution using a slip model.[2] Furthermore, the diffusion length $l_d=\sqrt{\mu\gamma}$ of the CH model, μ being a characteristic viscosity, shows a clear correspondence to the slip length l_s in the slip model. The difference between the CH and slip models mainly lies in the vicinity of the contact line within l_s or l_d. This is not surprising as Dussan V.[10] showed that the macroscopic flow is insensitive to the details of the slip model. Yue *et al.*[6] extracted an empirical criterion for achieving the sharp-interface limit, $\epsilon<4l_d$, which sets the maximum allowable interfacial thickness for simulating a physical system with diffusion length l_d. Thus, the sharp-interface limit seems to be firmly established for a CH description of moving contact lines.

However, two additional issues must be resolved before one can answer the question raised above. The first is a technical one on resolving the diffusion or slip length numerically. For real materials, the slip length l_s is exceedingly small. For glycerin displacing silicone oil in capillary tubes, Fermigier and Jenffer[11] estimated l_s to be less than 10 nm, consistent with newer and more accurate measurements.[12] This means that a diffuse-interface simulation, in order to achieve the sharp-interface limit, would have to use a comparable ϵ value. To capture the interfacial profile and hence

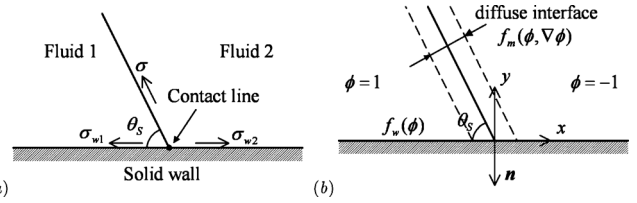

FIG. 1. A static contact line viewed in (a) the sharp-interface model and (b) the diffuse-interface model. $\boldsymbol{n}$ is the outward normal to the wall. The phase-field variable ϕ represents the two fluid bulks by $\phi=\pm 1$ and the fluid-fluid interface by $\phi=0$. Other symbols are defined in the text.

the interfacial tension accurately, the grid size needs to be at least as small as ϵ.[8,9] Thus, to simulate displacement in the 2 mm diameter capillary of Fermigier and Jenffer,[11] one must cover five or six decades of length scales, which is beyond the current computational capacity. This is analogous to the requirement in sharp-interface computations of resolving the slip length.[13,14]

The second issue concerns the equilibrium between the fluid components with the solid wall at the contact line. Most of the diffuse-interface studies so far have assumed instant equilibration between the fluid and the wall, thus neglecting the effect of nonequilibrium wall layers. As shown by Jacqmin,[3] such an effect can be accommodated by the CH model if one allows a finite relaxation of the fluid layer next to the wall. Qian *et al.*[15] included such relaxation in their computation of the Couette flow but did not examine its effect. The simulation of Carlson *et al.*[16] indicated that wall relaxation tends to inhibit the motion of the contact line and reduce the speed of drop spreading. But the mechanism for this is unclear. As an important aspect of the CH model for contact lines, wall relaxation remains largely unexplored.

This study aims to resolve these two issues. First, we elucidate the effect of wall relaxation on contact-line dynamics. A somewhat surprising finding is that wall relaxation and CH diffusion counteract each other in defining the macroscopic solution. Second, we exploit the antagonism to address the difficulty in resolving the small slip length. We propose a numerical strategy for attaining reliable solutions on the macroscopic length scale by solving the moving-contact-line problem with an artificially large l_d and a properly determined wall relaxation. The latter corrects the distortions to the solution caused by using the large l_d. Thus, we obtain an accurate simulation of a flow situation with very small slip or diffusion length at a manageable computational cost.

II. FORMULATIONS

Consider two immiscible fluids in contact with each other and with a solid surface (Fig. 1). In terms of the phase-field variable ϕ, the free energy of the fluid-wall system can be written as

$$\mathcal{F}=\int_{\Omega} f_m(\phi,\nabla\phi)d\Omega+\int_{\partial\Omega} f_w(\phi)dA, \tag{1}$$

where Ω is the fluid domain and $\partial\Omega$ is the solid surface. f_m is the fluid-fluid mixing energy,[17]

$$f_m(\phi,\nabla\phi)=\frac{\lambda}{2}|\nabla\phi|^2+\frac{\lambda}{4\epsilon^2}(\phi^2-1)^2, \tag{2}$$

and f_w is the wall energy,[3,18]

$$f_w(\phi)=-\sigma\cos\theta_S\frac{\phi(3-\phi^2)}{4}+\frac{\sigma_{w1}+\sigma_{w2}}{2}. \tag{3}$$

In f_m, λ is the mixing energy density, ϵ is the capillary width, and in equilibrium the fluid-fluid interfacial tension is given by

$$\sigma=\frac{2\sqrt{2}}{3}\frac{\lambda}{\epsilon}. \tag{4}$$

Note that the wall energy $f_w(\pm 1)$ gives the fluid-solid interfacial tension σ_{w1} and σ_{w2} for the two fluids, which determine the static contact angle θ_S through Young's equation $\sigma_{w2}-\sigma_{w1}=\sigma\cos\theta_S$.

A variational procedure leads to three interesting quantities:[3,19] the bulk chemical potential $G=\lambda[-\nabla^2\phi+(\phi^2-1)\phi/\epsilon^2]$, the surface chemical potential $L=\lambda\boldsymbol{n}\cdot\nabla\phi+f_w'(\phi)$, and a "body force" $\boldsymbol{B}=G\nabla\phi$ that is the diffuse-interface equivalent of the interfacial tension.[8] Now the moving contact line can be formulated as a boundary-value problem. The Navier–Stokes and Cahn–Hilliard equations read

$$\nabla\cdot\boldsymbol{v}=0, \tag{5}$$

$$\rho\left(\frac{\partial\boldsymbol{v}}{\partial t}+\boldsymbol{v}\cdot\nabla\boldsymbol{v}\right)=-\nabla p+\mu\Delta\boldsymbol{v}+G\nabla\phi, \tag{6}$$

$$\frac{\partial\phi}{\partial t}+\boldsymbol{v}\cdot\nabla\phi=\nabla\cdot(\gamma\nabla G). \tag{7}$$

The Cahn–Hilliard equation describes the convection-diffusion of the two fluids, with a diffusive flux proportional to the ∇G, the coefficient γ being the mobility parameter. The following boundary conditions apply on the solid substrate $\partial\Omega$:

$$\boldsymbol{v}=\boldsymbol{v}_w, \tag{8}$$

$$\boldsymbol{n}\cdot\nabla G=0, \tag{9}$$

$$\frac{\partial\phi}{\partial t}+\boldsymbol{v}\cdot\nabla\phi=-\Gamma L, \tag{10}$$

where $\boldsymbol{v}_w$ is the wall velocity. The no-slip boundary condition implies that the contact line moves only by means of CH diffusion across the interface. Jacqmin[20] and Qian *et al.*[5] introduced a slip velocity here that would give more freedom in fitting the data and perhaps also a better representation of the true physics. In view of our aim, however, we strive to minimize the number of parameters. The second condition asserts zero flux through the wall. The third allows relaxation of the wall layer as driven by the surface potential L, Γ being a rate constant.[3,5]

Thus, the CH model contains four model parameters: λ, ϵ, γ, and Γ. Of these, ϵ will be given a value small enough to achieve the sharp-interface limit, and λ is constrained by Eq. (4). The remaining two parameters will be the focus of this

work. Although one could view γ and Γ as material properties related to parameters in molecular-kinetic theory,[3,16] their values are not known for any specific fluid-solid combinations. Therefore, we will treat them as phenomenological parameters in the phenomenological Cahn–Hilliard model.

In the numerical simulations to be presented, we neglect inertia since it bears little on the aim of this study. The problem is thus governed by six dimensionless groups,

$$\mathrm{Ca} = \frac{\mu V}{\sigma} \quad \text{(capillary number)}, \tag{11}$$

$$\eta = \frac{\mu_r}{\mu} \quad \text{(viscosity ratio)}, \tag{12}$$

$$\mathrm{Cn} = \frac{\epsilon}{W} \quad \text{(Cahn number)}, \tag{13}$$

$$S = \frac{\sqrt{\gamma\mu}}{W}, \tag{14}$$

$$\Pi = \frac{1}{\mu\Gamma W}, \tag{15}$$

$$\theta_S \quad \text{(static contact angle)}, \tag{16}$$

where W is the macroscopic length scale, V is a velocity scale, and μ and μ_r are the viscosities of the advancing and receding fluid. In steady problems such as dynamic wetting of a capillary, V is simply the steadily moving-contact-line speed relative to the solid wall. In problems such as drop spreading, the contact-line velocity is part of the solution rather than a parameter, so will be Ca. Of note is the diffusion length $l_d=\sqrt{\gamma\mu}$, which is related directly to the slip length l_s in the sharp-interface limit.[21] Bulk diffusion and wall relaxation are embodied, respectively, by S and Π.

The computation uses Galerkin finite elements on an adaptive triangular grid that adequately resolves the interfacial region. The Navier–Stokes and Cahn–Hilliard equations are integrated using a second-order accurate, fully implicit time-marching scheme. Details of the numerical algorithm and validation can be found in Ref. 8.

III. RESULTS AND DISCUSSIONS

We will study two flows in this paper, the dynamic wetting in a circular capillary tube and spontaneous drop spreading (Fig. 2). The former is a steady problem and the reference frame is fixed to the contact line. Both problems are axisymmetric and only one half of the meridian plane is calculated. In Fig. 2(a), the tube radius is W and we calculate a tube length of $6W$ with a parabolic Poiseuille velocity profile imposed at the inlet and outlet. In Fig. 2(b), the computational domain extends $4R_0\times 4R_0$ on the meridian plane, with R_0 being the characteristic macroscopic length. Zero stress boundary condition is imposed on the outer boundaries.

A key observable of the problems is the apparent contact angle θ_A characterizing the fluid-fluid interface at the macroscopic length scale W. Its definition is not unique. For example, one can measure the interface angle at some distance to the contact line or use the angle formed by extrapolating the interface to the solid wall.[22] Various experiments[11,23–25] have adopted the latter scheme by assuming the interface in the bulk to be spherical, which is a good approximation for $\mathrm{Ca}\ll 1$. We take the same scheme to facilitate the comparison. In the Poiseuille flow, following Fermigier and Jenffer,[11] we fit the interface (the $\phi=0$ level set) to a circular arc and calculate θ_A by $\theta_A=\cos^{-1}(W/R)$, where R is the radius of the circular arc.

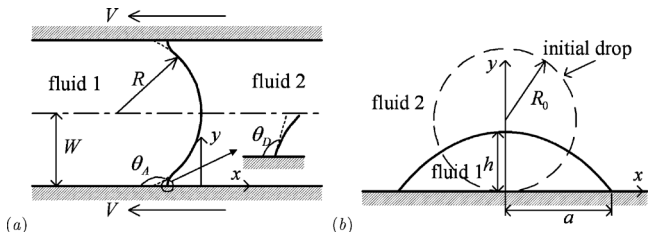

FIG. 2. Schematics of the computational setup. (a) Dynamic wetting of a capillary. (b) Spontaneous spreading of a drop on a partially wetting substrate. θ_D is the microscopic dynamic contact angle and θ_A is a suitably defined apparent contact angle.

A. Dynamic contact angle

From an asymptotic solution based on a slip length l_s, Cox[2] derived a celebrated formula for the apparent contact angle θ_A,

$$g(\theta_A) = g(\theta_S) + \mathrm{Ca}\,\ln\left(\frac{W}{l_s}\right), \tag{17}$$

where g is an algebraically complex function defined by Eqs. (3.21) and (7.11) of Cox.[2] It also depends on the viscosity ratio η, omitted from the above for brevity. Cox's solution assumes that during flow, the interface retains the equilibrium contact angle θ_S within the slip zone ($r\le l_s$), and the apparent contact angle is the result of viscous force bending the interface on a length scale $r\gg l_s$.

This formula underpredicts θ_A in liquid-liquid displacement in capillary tubes, not only for larger Ca, where it is expected to fail, but for small Ca as well.[11,13,26] Figure 3 illustrates a relatively benign case where there happens to be good agreement for the smallest Ca. Two *ad hoc* measures have been proposed to reduce the discrepancy. Fermigier and Jenffer[11] added an adjustable coefficient in front of Ca in Cox's formula, which effectively shifts the curve horizontally. The fitting improved somewhat (Fig. 3), but was still considered unsatisfactory. Zhou and Sheng,[13] among others, advocated the idea that surface roughness causes an additional viscous friction F on the interface that increases the viscous bending near the contact line. This is formulated by viewing θ_S of Eq. (17) not as the static contact angle, but as a microscopic *dynamic contact angle* θ_D that increases with the contact-line speed. Postulating $F/\sigma=\cos\theta_S-\cos\theta_D(\mathrm{Ca})=B(\mathrm{Ca})^x$, they were able to achieve close fitting by adjusting B and x for different data sets. In particular, x falls between 1/3 and 1/2.

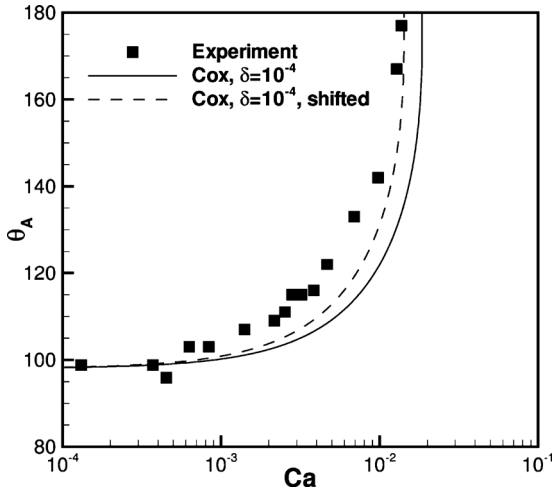

FIG. 3. Failure of the Cox formula to predict θ_A(Ca) for liquid-liquid displacement in a capillary tube. The symbols are experimental data for a glycerin-silicone oil system with θ_S=98° and receding-to-advancing viscosity ratio η=0.9. The solid line is the prediction of the Cox formula with $\delta=l_s/W=10^{-4}$, and the dashed line is the same prediction shifted to the left by multiplying Ca by a factor of 1.3 (or equivalently setting $\delta=10^{-5.2}$). Adapted from M. Fermigier and P. Jenffer (Ref. 11).

A notable feature of the CH model is that it does not assume a fixed $\theta_D=\theta_S$. Wall relaxation at a finite Γ causes θ_D to deviate from θ_S during flow. This deviation is a key idea in the molecular-kinetic model for the contact line[27] and is supported by molecular dynamics (MD) simulations.[15,28] In fact, a $\theta_D \sim$ Ca relationship can be derived analytically based on Eq. (10), the boundary condition for the Cahn–Hilliard equation.

We consider a steady slow flow (Ca$\ll$1) such that ϕ maintains its equilibrium hyperbolic tangent profile across the interface. The interface $\phi=0$ intersects the wall at the microscopic dynamic contact angle θ_D. Now Eq. (10) reduces to

$$\boldsymbol{v}\cdot\nabla\phi=-\Gamma[\lambda\boldsymbol{n}\cdot\nabla\phi+f_w'(\phi)], \tag{18}$$

which will be applied at the contact line. Denoting the value of $|\nabla\phi|$ at the center of the interface by ϕ_n, the left hand side can be expressed as

$$\text{LHS}=V\phi_n\sin\theta_D, \tag{19}$$

as $\boldsymbol{v}=(-V,0)$ on the wall, as shown in Fig. 2(a). The right hand side of Eq. (18) can be written as

$$\begin{aligned}\text{RHS}&=-\Gamma[(\lambda\boldsymbol{n}\cdot\nabla\phi)_D+f_w'(0)]\\&=-\Gamma[(\lambda\boldsymbol{n}\cdot\nabla\phi)_S+f_w'(0)+(\lambda\boldsymbol{n}\cdot\nabla\phi)_D\\&\quad-(\lambda\boldsymbol{n}\cdot\nabla\phi)_S]\\&=-\Gamma[(\lambda\boldsymbol{n}\cdot\nabla\phi)_D-(\lambda\boldsymbol{n}\cdot\nabla\phi)_S]\\&=-\Gamma\lambda\phi_n(\cos\theta_D-\cos\theta_S),\end{aligned} \tag{20}$$

where the subscripts S and D denote the static and dynamic states, and we have used $L(\phi,\nabla\phi)=(\lambda\boldsymbol{n}\cdot\nabla\phi)_S+f_w'(0)=0$ for a static contact line. Equating LHS and RHS gives

$$h(\theta_D,\theta_S)=\frac{\cos\theta_S-\cos\theta_D}{\sin\theta_D}=\frac{V}{\Gamma\lambda}=\left(\frac{2\sqrt{2}}{3}\frac{\Pi}{\text{Cn}}\right)\text{Ca}. \tag{21}$$

This simple equation has two significant ramifications. If $\Pi=0$, then θ_D remains at the static value θ_S as long as the flow is slow enough not to distort the equilibrium ϕ profile. This has been recognized by Jacqmin.[3] Furthermore, for small deviations of θ_D from θ_S, the above equation reduces to

$$\Delta\theta=\theta_D-\theta_S=\frac{V}{\Gamma\lambda}. \tag{22}$$

In the leading order, therefore, $\Delta\theta$ scales linearly with Ca in the CH model, rather than as $\text{Ca}^{1/3}$ or $\text{Ca}^{1/2}$.[13] Equation (22) is consistent with the scaling argument of Qian *et al.*[5] We have verified Eq. (21) numerically by varying θ_S, S, Π, and Ca systematically. Figure 4 shows that $h(\theta_D,\theta_S)$ indeed increases linearly with Ca with slopes closely approximating the analytical value. When $\Pi=0$, $\Delta\theta$ hovers around zero within the range (−0.7°, 2.3°). These small deviations from zero are mainly due to numerical errors in contouring ϕ.

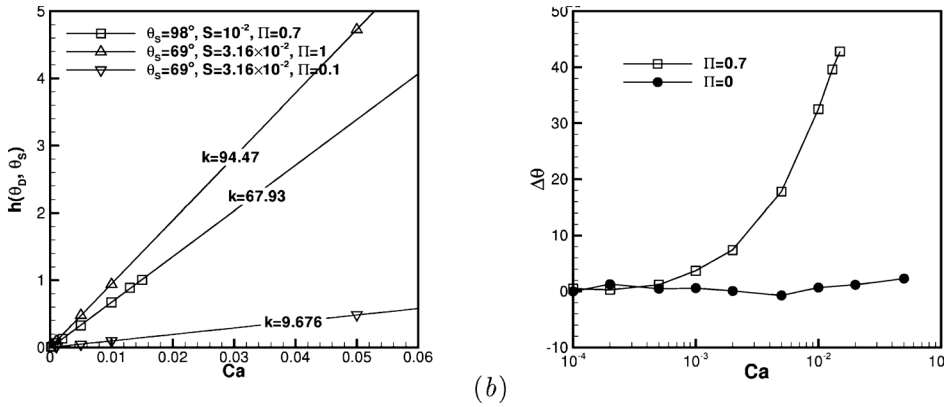

(a) (b)

FIG. 4. Deviation of the dynamic contact angle from the static one predicted by the CH model. (a) $h(\theta_D,\theta_S)$ as a function of Ca. The three sets of computations fall on straight lines of slope k. The analytical slopes are 94.28, 66.00, and 9.43, respectively. Cn=0.01. η=0.9 for the square symbols and η=0.01 for the others. (b) For one set of computations (θ_S=98°, η=0.9, S=0.01), $\Delta\theta$ is compared with a baseline case with Π=0.

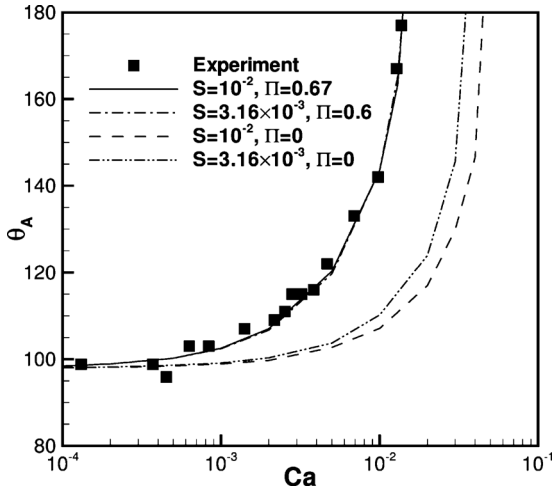

FIG. 5. Fitting the experimental data of Ref. 11 using Π as an adjustable parameter. The data are for glycerin displacing silicone oil in a capillary with $\theta_S=98°$, $\eta=0.9$. Cn=0.01 for the numerical curves. With $\Pi=0$, the model underpredicts the data by a wide margin.

B. Wall relaxation versus bulk diffusion

Does the CH model, aided by the dynamic contact angle of Eq. (21), improve the agreement with the experimental data of Fig. 3? To answer this question using numerical computation, one immediately runs into the difficulty of resolving a very small S or l_d. Estimating the slip length l_s in their experiment, Fermigier and Jenffer[11] put the upper bound at $\delta=l_s/W=10^{-4}$. According to Yue *et al.*,[6] this corresponds to a diffusion length $l_d=l_s/2.5=4\times10^{-5}W$, which is two orders of magnitude below the numerically resolvable length using conventional computing power. Figure 5 indicates that reducing l_d or S does bring the apparent contact angle θ_A closer to the data, but the gap in S cannot be bridged.

With a finite Π, the wall relaxation allows θ_D to change with flow, and this may bring the model prediction at *an artificially large S* closer to the data. We have selected Π by matching the critical Ca^c for wetting failure, at which $\theta_A\to180°$. This is simpler than fitting the entire data set, and Ca^c turns out to be very sensitive to Π. The data set in Fig. 5, due to Fermigier and Jenffer,[11] has $\mathrm{Ca}^c\approx1.37\times10^{-2}$. We have determined the best-fitting Π for two S values and plotted the fitting curves in Fig. 5. Both show excellent fitting to the experimental data. Note that fitting through Π works better than shifting the curves in Fig. 3; Π modulates the shape of the curve in the middle as well.

The fact that experimental data can be fitted equally well by more than one set of (S,Π) values hints at a competition between the two. This can be understood in a two-region picture. In the near-wall region, Γ governs the relaxation of ϕ. A fast relaxation (large Γ) returns the microscopic dynamic contact angle θ_D to the equilibrium θ_S, while a slow relaxation allows θ_D to deviate from θ_S when the local ϕ field is advected by external flow. This is the physical interpretation of Eq. (21). In our geometry, therefore, a larger Π (or small Γ) induces a larger θ_D and hence a larger θ_A away from the wall. One can think of Π as acting to "rotate" the interface in the near-wall region as if it is hinged at the contact line. In the outer region, interfacial diffusion is governed by γ. A larger γ (or larger S) tends to restore the ϕ profile faster against convection, and provides stronger resistance to "viscous bending" and provides a smaller θ_A. Thus, one may say that wall relaxation Γ provides resistance to contact-line rotation while "bulk diffusion" γ away from the wall promotes resistance to viscous bending of the contact line. Slow wall relaxation and fast bulk diffusion compensate each other.

Previous hydrodynamic models for the contact line, exemplified by Cox,[2] attribute θ_A solely to viscous bending and neglect wall relaxation that causes $\theta_D\neq\theta_S$. Molecular-kinetic models, originated by Blake and Haynes,[29] consider only local processes that modify θ_D and neglect viscous bending. The Cahn–Hilliard model includes both, and in a way integrates these hitherto parallel approaches to the contact-line problem.[27]

C. A computational strategy

We propose the following procedure for determining the CH model parameters when simulating moving contact lines. First, we pick the smallest manageable interfacial thickness (or Cahn number Cn). This is dictated by the fact that the interfacial profile requires some ten grid points for sufficient resolution,[8] and a thinner interface means a greater number of mesh points over the entire domain. Second, we choose a γ value such that $S\geq\mathrm{Cn}/4$ to achieve the sharp-interface limit.[6] Finally, we use one experimental data point for the apparent contact angle or contact-line speed to determine the wall relaxation Γ. We recommend using the critical capillary number for wetting failure for its sensitivity to Γ. Now the CH model can be used to compute moving contact lines for other Ca and geometries for the same fluid and substrate materials as have provided the data point.

This strategy exploits the competition between bulk diffusion (γ) and wall relaxation (Γ); the same interfacial morphology can be realized outside the immediate neighborhood of the contact line if both are strengthened or weakened in concert. Therefore, a simulation at a relatively large γ and a suitably chosen Γ can recover the correct macroscopic solution in a moving-contact-line experiment having a much smaller slip length. To present this idea more precisely, it is helpful to recall the classical two-region picture for the contact line:[10] an inner slip region and an outer region. The slip length being of molecular dimension, the inner slip region is inaccessible to measurement or continuum computation. It is only the outer solution that is of practical concern. In the matched solution of Cox,[2] an intermediate region is introduced for technical reasons, which is part of the outer solution for the present purpose. The same two-region picture can be borrowed into the CH solution, except that the length scale of the inner region, the diffusion length, will be artificially enlarged. Now it becomes necessary to distinguish the "real" and small slip length $\tilde{l}_s$ from the artificially large slip length $\bar{l}_s=2.5\bar{l}_d$ used in the CH computation. We will use a tilde to indicate quantities associated with the former and an overbar with the latter.

This idea has some historical origins. First, Dussan V.[10]

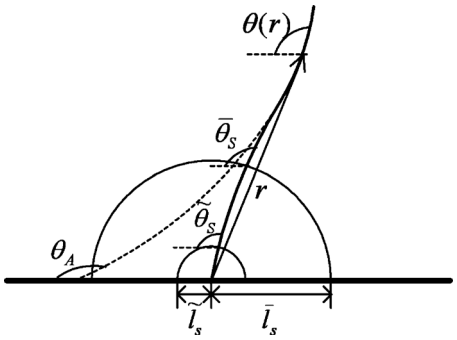

FIG. 6. Schematic illustrating the three contact angles $\tilde{\theta}_S$, $\bar{\theta}_S$, and θ_A evaluated at different length scales $\tilde{l}_s$, $\bar{l}_s$, and W. Note that θ_A is extracted from the static-like portion of the macroscopic interface.

showed that the outer solution is insensitive to the details inside the slip zone. Therefore, different slip models can be used to produce the same fluid dynamics on larger scales.[26] Then Ngan and Dussan V.[30] parametrized the boundary-value problem in the outer region in terms of an *intermediate contact angle*, different from $\tilde{\theta}_S$, measured at an intermediate distance (larger than $\tilde{l}_s$) from the contact line. Shen and Ruth[31] adopted this strategy in their finite-element calculations of moving contact lines between parallel plates and achieved good agreement with experiment. A similar approach was used by Afkhami *et al.*[32] in handling the contact angle associated with "numerical slip" based on the finite mesh size at the solid boundary. These can all be seen as "compensation strategies" that recover the correct macroscopic solution at lower cost by imposing a modified contact angle $\bar{\theta}_S$ along with a larger slip length $\bar{l}_s$ (Fig. 6).

Such a strategy can be justified rigorously by Cox's asymptotic solution[2] for vanishing Ca. Writing the intermediate solution at $\tilde{l}_s \ll r \ll W$ in terms of the inner variables, we have

$$g[\theta(r)] = g(\tilde{\theta}_S) + \mathrm{Ca}\,\ln\left(\frac{r}{\tilde{l}_s}\right), \tag{23}$$

which can be used to calculate the angle of the interface at an intermediate length $\bar{l}_s$,

$$g(\bar{\theta}_S) = g(\tilde{\theta}_S) + \mathrm{Ca}\,\ln\left(\frac{\bar{l}_s}{\tilde{l}_s}\right), \tag{24}$$

where $\bar{\theta}_S = \theta(\bar{l}_s)$. Subtracting the above two equations, we express the slope of the interface at any $\tilde{l}_s \ll r \ll W$ in terms of the length $\bar{l}_s$ and angle $\bar{\theta}_S$,

$$g[\theta(r)] = g(\bar{\theta}_S) + \mathrm{Ca}\,\ln\left(\frac{r}{\bar{l}_s}\right). \tag{25}$$

Matching the intermediate solution with the outer solution, we can also write the former as

$$g[\theta(r)] = g(\theta_A) + \mathrm{Ca}\,\ln\left(\frac{r}{W}\right). \tag{26}$$

The elimination of $g[\theta(r)]$ from Eqs. (23), (25), and (26) yields the apparent contact angle θ_A,

$$g(\theta_A) = g(\bar{\theta}_S) + \mathrm{Ca}\,\ln\left(\frac{W}{\bar{l}_s}\right) = g(\tilde{\theta}_S) + \mathrm{Ca}\,\ln\left(\frac{W}{\tilde{l}_s}\right), \tag{27}$$

which agrees with Cox's formula in Eq. (17). Equation (27) states that the outer solution can be parametrized in terms of an intermediate contact angle $\bar{\theta}_S$ and an intermediate slip length $\bar{l}_s$ that satisfy Eq. (24), which is what Ngan and Dussan V.[30] and Dussan V. *et al.*[33] suggested. Note that although $\bar{\theta}_S$ is the interface angle at $\bar{l}_s$, it is imposed on the wall in the parametrization of Ngan and Dussan V.[30] This is valid because the interface has little curvature inside the slip region,[2] and the distance $\bar{l}_s$ is infinitesimal when viewed from the outer solution.

The compensation idea can be borrowed into the CH framework by stipulating that $\bar{\theta}_S$ be given by the dynamic contact angle θ_D of Eq. (21). For a physical system with a diffusion length $\tilde{l}_d$ and wall relaxation constant $\tilde{\Gamma}$, a simulation using a larger $\bar{l}_d$ can reproduce the correct macroscopic solution if the wall relaxation is modified to $\bar{\Gamma}$, which will be determined by the requirement that $\theta_D = \bar{\theta}_S$ in the limit of vanishing Ca. To bypass the algebraic complexity of the function g, we adopt the approximation of Sheng and Zhou[26] of Eq. (24),

$$\cos(\tilde{\theta}_S) - \cos(\bar{\theta}_S) \approx 5.63\ \ \mathrm{Ca}\,\ln\left(\frac{\bar{l}_s}{\tilde{l}_s}\right), \tag{28}$$

which is accurate for moderate contact angles satisfying $|\cos\theta_S| < 0.6$ and matched viscosity. Comparing this equation with Eq. (21), we find that $\theta_D \approx \bar{\theta}_S$ for $\theta_D \sim 90°$ if $\bar{\Pi}$ is chosen such that

$$\frac{2\sqrt{2}}{3}\frac{\bar{\Pi} - \tilde{\Pi}}{\mathrm{Cn}} = 5.63\,\ln\left(\frac{\bar{l}_s}{\tilde{l}_s}\right) = 5.63\,\ln\left(\frac{\bar{l}_d}{\tilde{l}_d}\right), \tag{29}$$

where we have used the result of Yue *et al.*[6] that the slip length $l_s = 2.5 l_d$. This formula gives the amount of wall relaxation (or $\bar{\Gamma}$) that is needed to compensate for using an artificially large diffusion length (or $\bar{\gamma}$). Needless to say, the strategy hinges on the wide separation of the length scales $\tilde{l}_s$ and W, which is at the root of the numerical difficulty in resolving $\tilde{l}_s$. In light of this compensation scheme for the CH model, the data fitting in the proposed strategy is necessitated by the fact that the true slip length $\tilde{l}_s$ and relaxation parameter $\tilde{\Gamma}$ are not known for a specific experiment.

Equation (29) is confirmed by numerical results. The excellent fitting to experimental data in Fig. 5 was achieved by two pairs of (S,Π) values that satisfy Eq. (29); both correspond to an idealized state of $\tilde{l}_s/W = 3.4\times10^{-7}$ and $\tilde{\Pi} = 0$. This $\tilde{l}_s$ value is of molecular dimension, and smaller than that $(\tilde{l}_s/W = 10^{-6} - 10^{-5})$ used by Fermigier and Jenffer[11] to fit

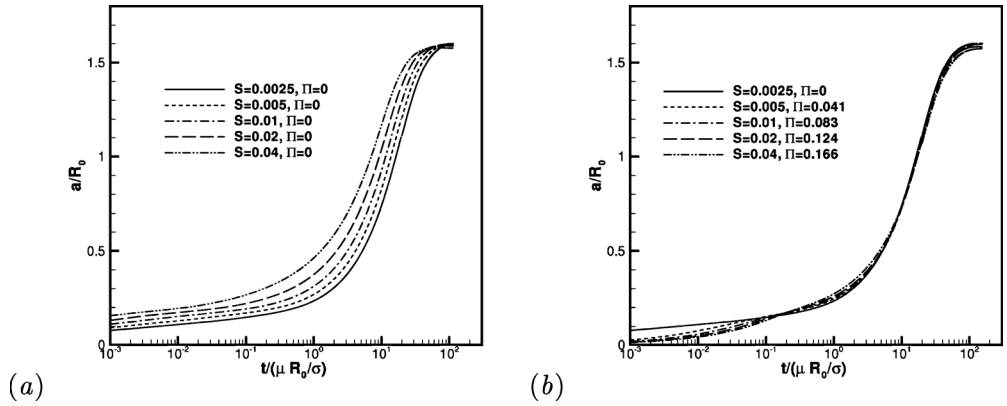

FIG. 7. Simulations of drop spreading on a partially wetting substrate with $\tilde{\theta}_S=60°$, $\eta=1$, Cn=0.01. (a) Increasing bulk diffusion S accelerates the spreading. (b) A universal spreading curve is achieved by using wall relaxation given by Eq. (29) to counter the bulk diffusion.

their data. Further validation comes from simulations of drop spreading on a partially wetting substrate. The geometry is shown in Figs. 2(b) and Fig. 7 plots the increase of the scaled contact-line radius a/R_0 in time. Without wall relaxation (a), a drop with a larger diffusion length (or S) spreads faster as expected. However, all the curves collapse into one in (b) if wall relaxation is included with Π values chosen according to Eq. (29). The discrepancies at the beginning are due to the fact that the system is far from equilibrium and the ϕ profile across the interface deviates from its hyperbolic tangent form. Interestingly, the success of Eq. (29) seems to go beyond the conditions assumed in its derivation. For instance, the fitting in Fig. 5 covers the entire Ca range, not only the limit of vanishing Ca. The dynamic contact angle in Fig. 7 varies between 60° and 180°, quite far from the required $\theta_D \sim 90°$.

The geometry of the drop spreading problem offers an opportunity to elucidate the role of wall energy relaxation in contact-line motion. With increasing Π, the slower wall relaxation acts to increase the dynamic contact angle and produce a sharper wedge of the fluid being displaced. This increases the dissipation in the wedge, not only through viscous friction, but also through diffusion of the species.[8] Thus, wall relaxation tends to slow down the spreading of drops as previously noted by Carlson *et al.*[16] Heuristically, one may also consider the spreading to be driven by the difference between the apparent and dynamic contact angles. Therefore, the drop spreads more slowly when wall relaxation increases the dynamic contact angle.

IV. SUMMARY

This work examines the wall relaxation in the Cahn–Hilliard model for a moving contact line. There are three main results:

(a) Wall relaxation during flow causes the dynamic contact angle to deviate from the equilibrium one. At the limit of small capillary number, an analytical relationship is derived for this deviation.
(b) Wall relaxation and interfacial diffusion away from the wall compete in determining the apparent contact angle. The former allows deviation of the wall layer from equilibrium that tends to rotate the interface at the contact line to increase the apparent contact angle. The latter strives to restore the fluid interface to equilibrium to counter viscous bending, thus reducing the apparent contact angle.
(c) A computational strategy is proposed that exploits this competition to address the difficulty in resolving the slip length that in reality is very small. By imposing the dynamic contact angle, which is effectively the interface angle at a larger distance from the contact line, one obtains an accurate macroscopic solution at lower cost.

Although we have derived a formula for the amount of wall relaxation required to compensate for a large diffusion length, it does not specify how large each parameter should be in a simulation. The recommended protocol calls for fitting a single experimental datum to determine the two parameters, wall relaxation constant Γ and Cahn–Hilliard mobility γ. This is tantamount to determining the true slip length l_s of the physical system. Therefore, the CH model is in essence similar to the slip models that leave l_s adjustable.[10,11] But it fits the data much better than the Cox model (cf. Fig. 3). From a modeling point of view, such *ad hoc* input is perhaps unavoidable since real physics at molecular scales has been replaced by phenomenology on the continuum level.

Finally, the compensation scheme for the Cahn–Hilliard model illustrates a connection to slip models such as Cox.[2] It is based on similar ideas for the slip model due to Ngan and Dussan V.[30] and others. The key element is equating the Cahn–Hilliard dynamic contact angle θ_D with the intermediate contact angle $\bar{\theta}_S$ of Ngan and Dussan V.[30] Previously, the Cahn–Hilliard theory has been related with the slip models via the correspondence between the diffusion and slip length: $l_s=2.5l_d$. The wall relaxation provides another connection.

ACKNOWLEDGMENTS

P.Y. acknowledges the support by NSF-DMS Contract No. 0907788. J.J.F. acknowledges the support by the Petroleum Research Fund, the Canada Research Chair program,

NSERC (Discovery, Accelerator and Strategic grants), and the Canadian Foundation for Innovation. The computation was done at WestGrid.

[1]F. Y. Kafka and E. B. Dussan V., "On the interpretation of dynamic contact angles in capillaries," J. Fluid Mech. **95**, 539 (1979).
[2]R. G. Cox, "The dynamics of the spreading of liquids on a solid surface. Part 1. Viscous flow," J. Fluid Mech. **168**, 169 (1986).
[3]D. Jacqmin, "Contact-line dynamics of a diffuse fluid interface," J. Fluid Mech. **402**, 57 (2000).
[4]L. M. Pismen, "Mesoscopic hydrodynamics of contact line motion," Colloids Surf., A **206**, 11 (2002).
[5]T. Qian, X.-P. Wang, and P. Sheng, "A variational approach to moving contact line hydrodynamics," J. Fluid Mech. **564**, 333 (2006).
[6]P. Yue, C. Zhou, and J. J. Feng, "Sharp-interface limit of the Cahn-Hilliard model for moving contact lines," J. Fluid Mech. **645**, 279 (2010).
[7]G. Caginalp and X. Chen, "Convergence of the phase field model to its sharp interface limits," Eur. J. Appl. Math. **9**, 417 (1998).
[8]P. Yue, C. Zhou, J. J. Feng, C. F. Ollivier-Gooch, and H. H. Hu, "Phase-field simulations of interfacial dynamics in viscoelastic fluids using finite elements with adaptive meshing," J. Comput. Phys. **219**, 47 (2006).
[9]C. Zhou, P. Yue, J. J. Feng, C. F. Ollivier-Gooch, and H. H. Hu, "3D phase-field simulations of interfacial dynamics in Newtonian and viscoelastic fluids," J. Comput. Phys. **229**, 498 (2010).
[10]E. B. Dussan V., "The moving contact line: The slip boundary condition," J. Fluid Mech. **77**, 665 (1976).
[11]M. Fermigier and P. Jenffer, "An experimental investigation of the dynamic contact angle in liquid-liquid systems," J. Colloid Interface Sci. **146**, 226 (1991).
[12]C. Cottin-Bizonne, A. Steinberger, B. Cross, O. Raccurt, and E. Charlaix, "Nanohydrodynamics: The intrinsic flow boundary condition on smooth surfaces," Langmuir **24**, 1165 (2008).
[13]M.-Y. Zhou and P. Sheng, "Dynamics of immiscible-fluid displacement in a capillary tube," Phys. Rev. Lett. **64**, 882 (1990).
[14]M. C. T. Wilson, J. L. Summers, Y. D. Shikhmurzaev, A. Clarke, and T. D. Blake, "Nonlocal hydrodynamic influence on the dynamic contact angle: Slip models versus experiment," Phys. Rev. E **73**, 041606 (2006).
[15]T. Qian, X.-P. Wang, and P. Sheng, "Molecular scale contact line hydrodynamics of immiscible flows," Phys. Rev. E **68**, 016306 (2003).
[16]A. Carlson, M. Do-Quang, and G. Amberg, "Modeling of dynamic wetting far from equilibrium," Phys. Fluids **21**, 121701 (2009).
[17]J. W. Cahn and J. E. Hilliard, "Free energy of a nonuniform system. I. Interfacial free energy," J. Chem. Phys. **28**, 258 (1958).
[18]J. W. Cahn, "Critical-point wetting," J. Chem. Phys. **66**, 3667 (1977).
[19]T. Qian, X.-P. Wang, and P. Sheng, "Molecular hydrodynamics of the moving contact line in two-phase immiscible flows," Comm. Comp. Phys. **1**, 1 (2006).
[20]D. Jacqmin, "Onset of wetting failure in liquid-liquid systems," J. Fluid Mech. **517**, 209 (2004).
[21]For large viscosity disparity between the two fluids, η enters l_d as well: $l_d=(\mu\gamma)^{1/2}\eta^{1/4}$ (Ref. 6). Since η is not of major interest in this study, for brevity we retain the simpler form for l_d in the rest of the paper.
[22]C. G. Ngan and E. B. Dussan V., "On the nature of the dynamic contact angle: An experimental study," J. Fluid Mech. **118**, 27 (1982).
[23]R. L. Hoffman, "A study of the advancing interface," J. Colloid Interface Sci. **50**, 228 (1975).
[24]R. T. Foister, "The kinetics of displacement wetting in liquid/liquid/solid systems," J. Colloid Interface Sci. **136**, 266 (1990).
[25]A. Zosel, "Studies of the wetting kinetics of liquid drops on solid surfaces," Colloid Polym. Sci. **271**, 680 (1993).
[26]P. Sheng and M. Zhou, "Immiscible-fluid displacement: Contact-line dynamics and the velocity-dependent capillary pressure," Phys. Rev. A **45**, 5694 (1992).
[27]T. D. Blake, "The physics of moving wetting lines," J. Colloid Interface Sci. **299**, 1 (2006).
[28]J. Koplik, J. R. Banavar, and J. F. Willemsen, "Molecular dynamics of Poiseuille flow and moving contact lines," Phys. Rev. Lett. **60**, 1282 (1988).
[29]T. D. Blake and J. M. Haynes, "Kinetics of liquid/liquid displacement," J. Colloid Interface Sci. **30**, 421 (1969).
[30]C. G. Ngan and E. B. Dussan V., "On the dynamics of liquid spreading on solid surfaces," J. Fluid Mech. **209**, 191 (1989).
[31]C. Shen and D. W. Ruth, "Experimental and numerical investigations of the interface profile close to a moving contact line," Phys. Fluids **10**, 789 (1998).
[32]S. Afkhami, S. Zaleski, and M. Bussmann, "A mesh-dependent model for applying dynamic contact angles to VOF simulations," J. Comput. Phys. **228**, 5370 (2009).
[33]E. B. Dussan V., E. Rame, and S. Garoff, "On identifying the appropriate boundary conditions at a moving contact line: An experimental investigation," J. Fluid Mech. **230**, 97 (1991).